Sensor Fusion of Force and Acceleration for Robot Force Control

Gámez García, Javier; Robertsson, Anders; Gómez Ortega, Juan; Johansson, Rolf

Published in:
Proceedings. 2004 IEEE/RSJ International Conference on Intelligent Robots and Systems, 2004. (IROS 2004).

DOI:
10.1109/IROS.2004.1389867

2004

Proceedings of 2004 IEEE/RSJ International Conference on
Intelligent Robots and Systems
September 28 - October 2, 2004, Sendai, Japan

Sensor Fusion of Force and Acceleration for Robot Force Control

Gámez García J.[‡], Robertsson A.[†], Gómez Ortega J.[‡], Johansson R.[†]

[†]Department of Automatic Control, Lund University, Lund, Sweden.
e-mail: {Anders.Robertsson, Rolf.Johansson}@control.lth.se

[‡] System Engineering and Automation Department, Jaen University, Jaen, Spain.
e-mail: {jggarcia, juango}@ujaen.es

Abstract—**In this paper, robotic sensor fusion of acceleration and force measurement is considered. We discuss the problem of using accelerometers close to the end-effectors of robotic manipulators and how it may improve the force control performance. We introduce a new model-based observer approach to sensor fusion of information from various different sensors. During contact transition, accelerometers and force sensors play a very important role and it can overcome many of the difficulties of uncertain models and unknown environments, which limit the domain of application of currents robots used without external sensory feedback. A model of the robot-grinding tool using the new sensors was obtained by system identification. An impedance control scheme was proposed to verify the improvement. The experiments were carried out on an ABB industrial robot with open control system architecture.**

Keywords: **Force Control, Observers, Sensor Fusion, Impedance Control, Robot Control.**

I. Introduction

It is well known that for a robotic manipulator without sensors on the end-effector, the end-effector has to follow a path in its workspace without regard to any feedback other than its joints shaft encoder or resolvers. This fact imposes severe limitations on certain tasks where an interaction between the robot and the environment is needed. However, with the help of sensors, a robot can exhibit an "adaptive behavior" [2], the robot being able to deal flexibly with changes in its environment and to execute complicated skilled tasks.

Robot manipulator contact task execution represents an important problem as many tasks exist in which the robot is required to make intentional contact with fixed objects in the robot's work environment. These tasks include grinding, deburring and drilling, to name a few.

Whereas force sensor may be used to achieve force control, force sensors may have drawbacks if used in harsh environments and their measurements complex because they reflect forces other than contact forces such as inertial forces. Furthermore, there can be large benefits combining force estimates from model based observers with force and acceleration measurements in work with heavy tools in force interaction with the environment [5].

The problem formulation is as follows. When we want to get into contact with a surface using the end-effector of a robotic manipulator, the force sensor measures two kinds of forces: the environmental or contact force (F) and the inertial force produced by acceleration ($m\ddot{x}$), that is:

$$u = F + m\ddot{x} \tag{1}$$

Usually, the task undertaken requires the control of the force F.

The main contribution of this paper is the proposition of a new fusion of force and acceleration sensors into robot systems using an observer based in a Kalman Filter which combines the mentioned sensors with the goal of obtaining a suitable environmental force estimator. We focus on a robotic manipulator at which we have coupled two sensors on the end-effector, namely: a six-DOF wrist force sensor JR3® and one accelerometer to measure the acceleration, both are read in real time at the control level.

To verify the observer proposed, *impedance control* has been used [5]. It offers the possibility of controlling the dynamic relation between position of the robot tip and force exerted with the same control loop. The impedance relationship between force (F) and position (x) used in this paper is represented by the equation

$$F(t) = K_z x(t) + D_z \dot{x}(t) \tag{2}$$

where the positive gains K_z and D_z represent design parameters for stiffness and damping, respectively. Then, making the following impedance variable Z(s) converge to zero we can control the system [5].

$$Z(s) = K_z x(s) + D_z s x(s) - F(s) \tag{3}$$

This paper is structured as follows. In Section II the contact force observer is presented. In Sec. III, we describe the experimental setup and the sensing system. In Sec. IV, modeling of the system and the sensor fusion developed

0-7803-8463-6/04/$20.00 ©2004 IEEE

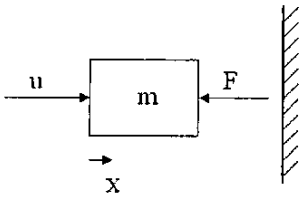

Fig. 1. Force interaction in the grinding tool mass simplified to design the observer.

is described. Section V shows some results obtained with the simulations and the experiments. Finally, we present the discussion and the conclusions in Sections VI and VII, respectively.

II. Force Observers

The objective of the force observer is to estimate the environmental force, that is, to separate the external forces and distal end-effector inertia forces in the measurement given by the force sensor. From Fig. 1, denoting the state of motion $\xi = (\xi_1, \xi_2)^T = (x, \dot{x})^T$, Eq. (2) can be rewritten as

$$m\ddot{\xi}_1 = u - F \tag{4}$$

where F is the unknown environmental force, u is the force measurement from the JR3 sensor and ξ_1 is the position of the tool. Writing Eq. (4) in state space form, we have

$$\frac{d}{dt}\begin{pmatrix}\xi_1\\ \xi_2\end{pmatrix} = \begin{pmatrix}0 & 1\\ 0 & 0\end{pmatrix}\begin{pmatrix}\xi_1\\ \xi_2\end{pmatrix} + \begin{pmatrix}0 & 0\\ \frac{1}{m} & \frac{-1}{m}\end{pmatrix}\begin{pmatrix}u\\ F\end{pmatrix} \tag{5}$$

As position, acceleration and force are assumed to be available to measurement, the outputs y of our system description may be arranged as

$$y = \begin{pmatrix}c_1\xi_1\\ c_2\ddot{\xi}_1 + c_3F\\ c_4\ddot{\xi}_1\end{pmatrix} = \begin{pmatrix}c_1 & 0 & 0\\ 0 & c_3 & c_2\\ 0 & 0 & c_4\end{pmatrix}\begin{pmatrix}\xi_1\\ F\\ \ddot{\xi}_1\end{pmatrix} \tag{6}$$

or

$$y = \begin{pmatrix}c_1 & 0\\ 0 & 0\\ 0 & 0\end{pmatrix}\begin{pmatrix}\xi_1\\ \xi_2\end{pmatrix} + \begin{pmatrix}0 & 0\\ \frac{c_2}{m} & c_3 - \frac{c_2}{m}\\ \frac{c_4}{m} & \frac{-c_4}{m}\end{pmatrix}\begin{pmatrix}u\\ F\end{pmatrix} \tag{7}$$

where all outputs are multiplied by a configurable gain c_i to be calibrated. In brief notation, we have

$$y = C\xi + D\begin{pmatrix}u\\ F\end{pmatrix} \tag{8}$$

Static Force Observers

A force observer suggested from these relationships would be

$$\begin{aligned}\widehat{F} &= D^{\dagger}y = \begin{pmatrix}0 & 1\end{pmatrix}\begin{pmatrix}\frac{c_2}{m} & c_3 - \frac{c_2}{m}\\ \frac{c_4}{m} & \frac{-c_4}{m}\end{pmatrix}^{-1}\begin{pmatrix}0 & 1 & 0\\ 0 & 0 & 1\end{pmatrix}y\\ &= \frac{1}{c_3c_4}\begin{pmatrix}0 & c_4 & -c_2\end{pmatrix}y\end{aligned} \tag{9}$$

Provided that the calibration constants $\{c_i\}_{i=1}^4$ are known and non-zero, the observer will offer an exact measurement of the force F without any observer dynamics. A direct calculation gives

$$\widehat{F} = \frac{1}{c_3c_4}\begin{pmatrix}0 & c_4 & -c_2\end{pmatrix}y = F \tag{10}$$

Dynamic Force Observers

Converting the equations of motion into a standard state space formulation, we have

$$\begin{cases}\dot{\xi} = A\xi + B(u - F)\\ y = C\xi + D_u u + D_F F\end{cases} \tag{11}$$

where the matrices A, B, C, D_u and D_F can be obtained from Eqs. (7) and (5) as

$$A = \begin{pmatrix}0 & 1\\ 0 & 0\end{pmatrix}, B = \begin{pmatrix}0\\ \frac{1}{m}\end{pmatrix} \tag{12}$$

$$C = \begin{pmatrix}c_1 & 0\\ 0 & 0\\ 0 & 0\end{pmatrix}, D_u = \begin{pmatrix}0\\ \frac{c_2}{m}\\ \frac{c_4}{m}\end{pmatrix}, D_F = \begin{pmatrix}0\\ c_3 - \frac{c_2}{m}\\ \frac{-c_4}{m}\end{pmatrix}$$

As previously mentioned, a Kalman filter is proposed to estimate the environmental force in system (11). In this context, an observer is used where the input F has not been considered and the resultant bias between data and Kalman filter output is instrumental for estimation of external forces acting on the system

$$\begin{cases}\dot{\widehat{\xi}} = A\widehat{\xi} + Bu + K(y - \hat{y})\\ \hat{y} = C\widehat{\xi} + D_u u\end{cases} \tag{13}$$

where $\widehat{\xi}$ corresponds to the ξ estimation being $\widehat{\xi} = (\widehat{\xi}_1\widehat{\xi}_2)^T$ and with the gain matrix

$$K = \begin{pmatrix}k_{11} & k_{12} & k_{13}\\ k_{21} & k_{22} & k_{23}\end{pmatrix} \tag{14}$$

The dynamics of the estimation error $\widetilde{\xi} = \xi - \widehat{\xi}$ are obtained as

$$\dot{\widetilde{\xi}} = (A - KC)\widetilde{\xi} - (B + KD_F)F \tag{15}$$

$$\widetilde{y} = y - \hat{y} = C\widetilde{\xi} + D_F F \tag{16}$$

Then, if the matrix $A - KC$ has eigenvalues with negative real part so that the observer be stable, an observer-based dynamic force observer may be suggested as

$$\widehat{F} = D_F^{\dagger}(C\widetilde{\xi} - \widetilde{y}) \tag{17}$$

with the property

$$\widehat{F} = D_F^{\dagger}(-C\widetilde{\xi} + \widetilde{y}) = D_F^{\dagger}D_F F = F \tag{18}$$

In the case studied here where $D_F^{\dagger}C = 0$, a particularly simple form of an unbiased force observer is obtained as

$$\widehat{F} = D_F^{\dagger}\widetilde{y} \tag{19}$$

Stochastic Force Estimation Error Dynamics

In the case where stochastic disturbances are present, we consider the system dynamics

$$\begin{cases} \dot{\xi} = A\xi + B(u-F) + v_x \\ y = C\xi + D_u u + D_F F + v_y \end{cases} \tag{20}$$

with

$$\mathcal{E}\{\begin{pmatrix} v_x \\ v_y \end{pmatrix}\} = 0, \quad \mathcal{E}\{\begin{pmatrix} v_x \\ v_y \end{pmatrix}\begin{pmatrix} v_x \\ v_y \end{pmatrix}^T\} = Q = \begin{pmatrix} Q_{xx} & Q_{xy} \\ Q_{yx} & Q_{yy} \end{pmatrix}$$

The stochastic properties of the static and dynamic force estimation errors $\tilde{F}$, respectively, will be

$$\tilde{F} = F - \hat{F} = F - D^{\dagger}y = -D^{\dagger}v_y \tag{21}$$

$$\mathcal{E}\{\tilde{F}\} = 0, \quad \mathcal{E}\{\tilde{F}\tilde{F}^T\} = D^{\dagger}Q(D^{\dagger})^T \tag{22}$$

and

$$\tilde{F} = F - \hat{F} = F - D_F^{\dagger}(\tilde{y} - C\tilde{\xi}) = -D_F^{\dagger}v_y \tag{23}$$

$$\mathcal{E}\{\tilde{F}\} = 0, \quad \mathcal{E}\{\tilde{F}\tilde{F}^T\} = D_F^{\dagger}Q(D_F^{\dagger})^T \tag{24}$$

Using transfer function notation, we have

$$\hat{F}(s) = D_F^{\dagger}[-C(sI - A + KC)^{-1}(B + KD_F) + D_F]F(s) + D_F^{\dagger}v_y(s) \tag{25}$$

$$= F(s) + D_F^{\dagger}v_y(s) \tag{26}$$

Whereas these force estimators are unbiased, they are sensitive to accelerometer noise and it is worthwhile to consider other force observer structures with low-pass properties.

Low-pass Force Observer Structures

As the unbiased force estimators are sensitive to accelerometer noise, it is worthwhile to consider other force observer structures with low-pass properties. In search of such observer structures, component-wise application of the observer (15) gives

$$\dot{\tilde{\xi}}_1 = -k_{11}c_1\tilde{\xi}_1 + \tilde{\xi}_2 + k_{11}c_1\xi_1 + \frac{k_{12}c_2 + k_{13}c_4}{m}u - K_1 y \tag{27}$$

$$\dot{\tilde{\xi}}_2 = -k_{21}c_1\tilde{\xi}_1 + k_{21}c_1\xi_1 - \frac{1}{m}F + \frac{k_{22}c_2 + k_{23}c_4}{m}u - K_2 y$$

Using Eq. (27), an expression for the dynamics of $\tilde{\xi}_1$ can be found as

$$\ddot{\tilde{\xi}}_1 + \Lambda_1\dot{\tilde{\xi}}_1 + \Lambda_0\tilde{\xi}_1 = \frac{-1}{m}F + \beta \tag{28}$$

with

$$\beta = k_{21}c_1\xi_1 + \frac{k_{22}c_2 + k_{23}c_4}{m}u - K_2 y$$

$$\Lambda_1 = k_{11}c_1, \qquad \Lambda_0 = k_{21}c_1 \tag{29}$$

Then, for slowly time-varying environmental forces F, it is possible to obtain an estimate $\hat{F}$ as

$$\hat{F} = m(\beta - \Lambda_0\tilde{\xi}_1) \tag{30}$$

Defining the force estimation error as $\tilde{F} = F - \hat{F}$ and considering Eqs. (15) and (30), the observer dynamics may be summarized as the state space system:

$$\begin{cases} \dot{\tilde{\xi}} = (A - KC)\tilde{\xi} - BF + KD_u u - Ky \\ \tilde{F} = F - m(\beta - \Lambda_0\tilde{\xi}_1) \end{cases} \tag{31}$$

where F is the input and $\tilde{F}$ is the output. The transfer function from F to $\tilde{F}$ is:

$$\tilde{F}(s) = \frac{s(s + k_{11}C_1)}{s^2 + k_{11}c_1 s + k_{21}c_1}(\beta - \frac{1}{m}F) = H(s)(\beta - \frac{1}{m}F) \tag{32}$$

where $H(s)$ is a strictly stable transfer function for all $k_{11} > 0$ and $k_{21} > 0$. It has one zero at $s = 0$ which shows that the force estimation error converges to zero for constant environmental forces. Moreover, the parameters Λ_i and β contain all the information about the behavior of $\hat{F}$; and, according to (28), by choosing appropriate observer gains k_{ij}, it is possible to shape these dynamics. Using Eqs. (30) and (28), we calculate the estimated force as

$$\hat{F} = m(-k_{21}c_1\dot{\hat{\xi}}_1 + k_{21}c_1\xi_1 + k_2 D_{F1}u - k_2 y) \tag{33}$$

where using (6), $c_2 = m$ and the rest of $c_i = 1$ we obtain

$$\hat{F} = k_{23}u - k_{23}m\ddot{\tilde{\xi}}_1 - k_{21}m\dot{\tilde{\xi}}_1 \tag{34}$$

In order to provide suitable values for k_{ij}, we note that when $\tilde{\xi}_1$ converges to zero according to specified dynamics, then it is suitable that Eq. (34) fulfills Newton's second law expressed in Eq. (4) thus imposing the following condition

$$k_{23} = 1 \tag{35}$$

III. Experimental Set-up

The robot-tool system is composed of the following devices and sensors (Fig. 2): an ABB robot; a wrist force sensor; a compliant grinding tool—*i.e.*, a device called Optidrive® that links the robot tip and the tool offering a compliant response—and, finally, an accelerometer. Fig. 3 shows a scheme of the system.

The robotic system used in this experiment was based on an ABB robot (Irb 2400) situated in the Robotics Lab at the Department of Automatic Control, Lund University. A totally open architecture is its main characteristic, permitting the implementation and evaluation of advanced control strategies. The controller was implemented in Matlab/Simulink using the Real Time Workshop of Matlab, and later compiled and linked to the Open Robot Control System [8]. The wrist sensor used was a DSP-based force/torque sensor of six degrees of freedom from JR3. The tool used for our experiments was a grinding tool with a weight of 12 kg. The mechanical device Optidrive—in itself a linear force sensor—the purpose of which was to provide to the tool additional damping contact with the environment, was considered

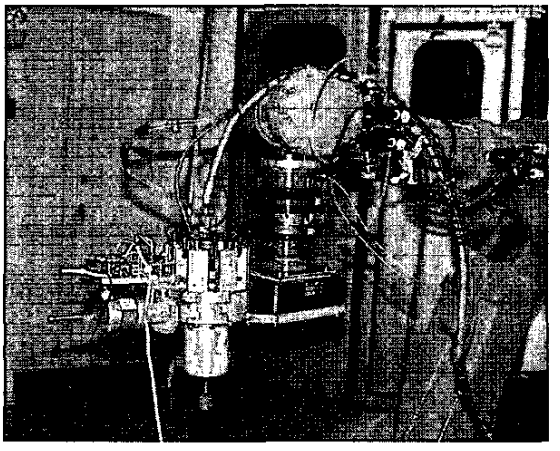

Fig. 2. The experimental setup. An ABB industrial robot IRB 2400 with an open control architecture system is used. The impedance control is performed perpendicular to the screen. Whereas the accelerometer is placed on the grinding tool, the Optidrive is placed between the tool and the JR3 sensor.

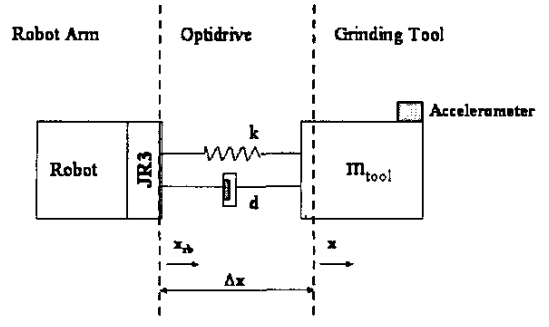

Fig. 3. Schematic robot-tool system with force sensor fusion where x_{rb} represents the position of the robot end-effector tip, x is the position of the tool and Δx is the distance between them

as a spring-damping system and provided a measure of the force exerted between its extremes. In this sense, the variable ΔX was indirectly measured through this force. The accelerometer was placed on the tip of the tool to measure its acceleration. The accelerometer and Optidrive signals were read by the robot controller in real time via an analog input.

For the environment, a vertical screen made of cardboard was used to represent the physical constraint (Fig. 4). The situation was modelled as a regular linear spring with

$$F = \begin{cases} 0 & \text{if } x \le x_c \\ k_{stiff}(x - x_c) & \text{if } x > x_c \end{cases}$$

The stiffness of the screen, k_{stiff}, was determined experimentally with a value of 5 N/mm. The impedance was controlled in the direction perpendicular to this screen, in the x direction of the robot system. From the impedance relationship, the stationary position depend on the relation

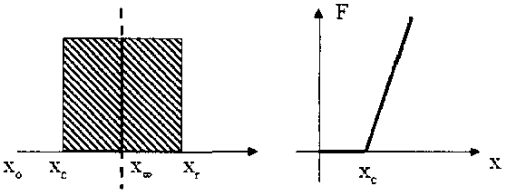

Fig. 4. a) A screen representing a physical constraint where x_c is the location of the screen, x_∞ the stationary position, and x_r the desired position in case of unconstrained motion (left). When the robot was in contact with the environment, the contact force was modelled as a linear spring. Without contact (right), the force was zero.

between the environmental stiffness and the robot stiffness. If stiff robot control was to be accomplished, then x_∞ must be chosen close to x_r, whereas a stiff environment lead to x_∞ being close to x_c [5].

IV. Modeling and Identification

The model used to design the impedance controller, which included the robot and the Optidrive grinding tool subsystem, was considered using only one cartesian direction (x) of the robot which corresponds with the tool compliance (Fig. 3). As the system was composed by the robot and the tool with the Optidrive device, it was necessary to obtain the dynamics of both subsystems. Previously, the calibration of the accelerometer and the Optidrive were done using the JR3 force sensor. For the experiment needed for the modeling of the accelerometer, the compliance of the Optidrive device was blocked. Using the acceleration estimation calculated from the robot kinematics and its position sensors, and the acceleration measured by the accelerometer, a model was estimated to finally calibrate the sensor. The model proposed was an output-error model

$$\mathcal{M}: \qquad y_k = \frac{B(q)}{F(q)} u_k + e_k \tag{36}$$

where k is sample index, q is the forward shift operator ($h = 4$ ms), $\{e_k\}$ normally distributed white noise and

$$B(q) = 4.0483 - 7.3764q^{-1} + 3.5761q^{-2};$$
$$F(q) = 1 - 2.1657q^{-1} + 1.6729q^{-2} - 0.4425q^{-3};$$

where the parameters were estimated using a prediction error method [4] and the Matlab System Identification Toolbox [7]. Figure 5 shows the agreement between the measured acceleration data and the estimated model output of the robot.

With respect to the robot, a linear dynamic model showing the relation between the position reference (x_r) and the current position of the robot tip (x_{rb}) (Fig. 3) was identified. An output-error model was calculated using the System Identification Toolbox of Matlab, the resulting model being as follows:

$$G_1(q) = \frac{1.2348q^{-1} - 1.5084q^{-2} + 0.3011q^{-3}}{1 - 1.0494q^{-1} + 0.0775q^{-2} - 0.0006q^{-3}} \tag{37}$$

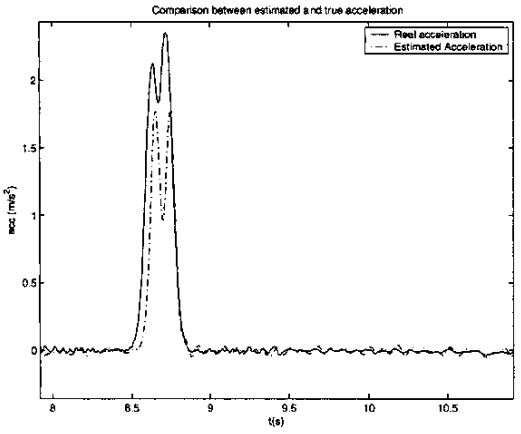

Fig. 5. Comparison between the acceleration obtained using the robot (solid) and the estimated acceleration (dashed) obtained using the accelerometer. The same input is used for both signals.

On the other hand, the transfer function of the Optidrive-tool subsystem that relates x with x_{rb} can be written as:

$$G_2(s) = \frac{k+ds}{m_{tool}s^2+ds+k} \tag{38}$$

where m_{tool} is the equivalent mass, that is, this mass includes the mass of the Optidrive, the accelerometer mass and the grinding tool ($m_{tool} = m_{grinder} + m_{accelerometer} + m_{Optidrive}$).

In order to estimate the parameters of G_2—that is, m_{tool}, the Optidrive stiffness k, and damping d—a least-squares approach was used. Then, considering the whole system model (*i.e.*, robot, tool and sensors) and using (37) and (38), the state space equations of the system were:

$$\begin{cases} \dot{x} = Ax + Bx_r \\ y = Cx \end{cases} \tag{39}$$

where $X = [\ddot{x}_{rb}, \dot{x}_{rb}, x_{rb}, x, \dot{x}]^T$ and

$$A = \begin{pmatrix} 49.6 & -55.8 & 0.4 & 0 & 0 \\ 658 & 641 & 4.8 & 0 & 0 \\ -8022 & 9077.2 & -1263 & 0 & 0 \\ 0 & 0 & 0 & 0 & 1 \\ 0 & d/m_{tool} & k/m_{tool} & -k/m_{tool} & -d/m_{tool} \end{pmatrix}$$

$$B = \begin{pmatrix} 214 \\ -444 \\ 7578 \\ 0 \\ 0 \end{pmatrix}, C = \begin{pmatrix} 1.2348 & -1.5084 & 0.3011 & 0 & 0 \\ 0 & 0 & 0 & 1 & 0 \end{pmatrix}$$

V. Simulations and Experiments

The impedance control approach was chosen as the control law to verify the improvement in force control performance using the force observer designed. In this sense, a LQR controller was used to make the relation of impedance proposed in (3) goes to zero [5]. The control law applied was

$$u = -LX + c\widehat{F} + l_r x_r \tag{40}$$

with c as the force gain in the impedance control, $\widehat{F}$ the estimated environmental force, which in our case it was estimated using the force observer, x_r the position reference and l_r the position gain constant, L being calculated considering (39).

The matrices Q and R representing penalties on the states and the control signal were chosen as

$$Q = \begin{pmatrix} 0.01 & 0 & 0 & 0 & 0 \\ 0 & D_r & 0 & 0 & 0 \\ 0 & 0 & K_r & 0 & 0 \\ 0 & 0 & 0 & K_t & 0 \\ 0 & 0 & 0 & 0 & D_t \end{pmatrix} \qquad R = 1000 \tag{41}$$

These choices were made considering that K_r and D_r affect the stiffness and the damping of the robot in the impedance relation and K_t and D_t related to the stiffness and the damping of the tool. Specific parameters values for our experiments were $K_r = 10$; $K_t = 10$; $D_r = 1$; $D_t = 1$.

To estimate the acceleration and velocity of the robot, an observer was developed [5]. For the force observer, an appropriate gain K was chosen following the restriction (35) and the conditions Λ_1, $\Lambda_0 \geq 0$. Then, the gains were selected as $k_{11} = 0.38$; $k_{12} = 0$; $k_{13} = -0.0073$; $k_{21} = 9.05$; $k_{22} = 0$; $k_{23} = 1$. The gain matrix L was calculated using (39) and (41), obtaining a value L = [0.0127 -0.0034 -0.0002 0.0080 0.0074]. The gain l_r results equal to 1.23.

For the experiment, the controller was implemented on an open robot control architecture with a sample time of 4 ms [8]. The simulations as well as the experiments carried out consisted of three phases: an initial movement in free space, a contact transition, and later, a movement in constrained space. The simulation of the experiment using the force observer is shown in Fig. 6 which shows how the observer avoids the inertial force at the beginning of the movement. The experiment on the real robot is shown in Fig. 7 which depicts, at the top, the force measurement from the JR3 sensor (left) and the force observer output (right) while at the bottom, the acceleration of the tool getting in contact with the environment (left), and the observer compensation (right) are shown. The robot position during this experiment is shown in Fig. 8.

VI. Discussion

In the experimental results, it is appreciated how the observer avoids the inertial force produced when the robot starts the movement (Fig. 7 at $t = 7.8s$) and also when the end-effector tip got into contact (Fig. 7 at $t = 8.5s$).

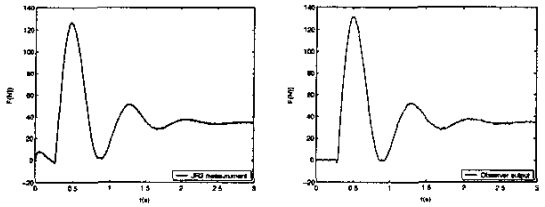

Fig. 6. Simulation of the JR3 measurement (left) and the force observer output (right). Note how the observer avoids the inertial effects for $t < 0.3s$ ($x_c = 50$ and $x_r = 80$).

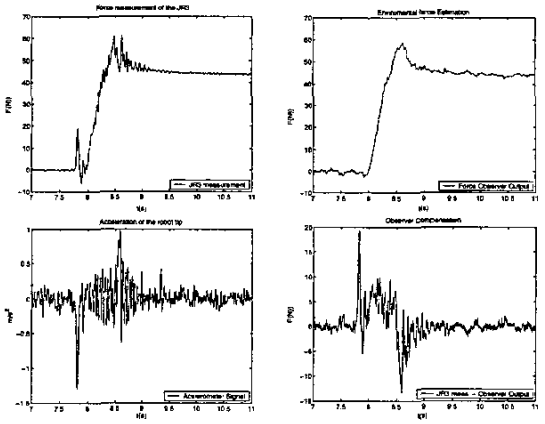

Fig. 7. Force measurement from the wrist sensor JR3 (upper-left), force observer output (upper-right). Acceleration of the robot tip (lower-left) and observer compensation (lower-right). The robot get into contact at $t = 8s$. It is appreciated how the observer eliminates the inertial effects ($t = 7.8s$ and $t = 8.5s$) and the noise introduced by the sensors.

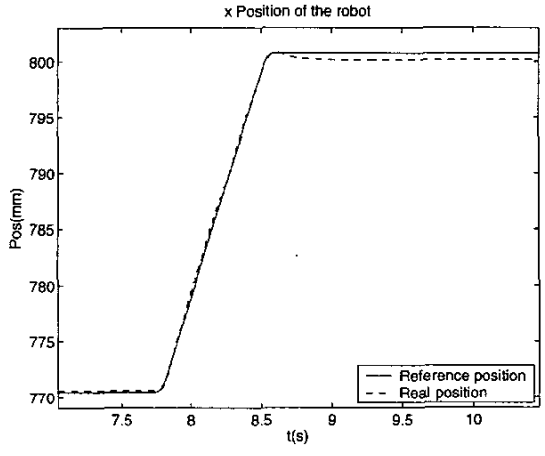

Fig. 8. Reference and real position of the robot during the experiment using the force observer information to execute the impedance control. The screen is situated in $x = 780$.

As the accelerometer was affected by the robot resonance (Fig. 7 (lower-left)), it must be pointed out that with simple addition of accelerometer sensors we would have a final signal with too much noise. The solution presented in this work for this aspect reduced this problem but the selection of the observer gains requires a trade off between the noise of the output and a fast response of our observer output. Finally, for appropriate choice of coefficients with an interesting result of this observer shown in Eq. (34), it can be seen that for a position estimated error equal to zero, the force observer fulfills Newton's second law where F would be the contact force.

VII. Conclusions

To estimate properly the environmental force in situations where the robot works in either free and constrained space, a force observer that takes into account the external forces, the position of the tool and the acceleration measurements at the end of the tool has been developed.

The main goal of the proposed force observer was to have an environmental force estimation permitting design of force control where the inertial forces do not interfere. This fact implies the improvement of the performance of the transition stage where the robot tasks leads to a contact between the robot tool and the environment. To verify the behavior of the observer simulations and experiments with an industrial robot were done.

Acknowledgment

The authors would like to acknowledge the Spanish CYCIT and MEC and the European Commission for partially funding this work under grants DPI2001-2424-C02-02, API2001-2337, Autofett and NACO2, respectively.

The authors are grateful to Tomas Olsson for experimental support.

References

[1] A. Alcocer, A. Robertsson, A. Valera and R. Johansson, *Force Estimation and Control in Robot Manipulators*. In Proc. 7th Symp. Robot Control (SYROCO'03), Sept. 1-3, pp. 31-36, Wroclaw, Poland, September 2003.

[2] F. Harashima and Y. Dote, *"Sensor Based Robot Systems"*. In Proc. IEEE Int. Workshop on Intelligent Motion COntrol, pp. 1-10, Istanbul, Turkey, August 1990.

[3] D. Henriksson, *"Observer-based Impedance Control in Robotics"*. Master Thesis. Dept. Automatic Control, Lund University, 2000.

[4] R. Johansson, *System Modeling and Identification*. Prentice Hall, Englewood Cliffs, NJ, 1993.

[5] R. Johansson and A. Robertsson. *Robotic Force Control using Observer-based Strict Positive Real Impedance Control*. In Proc. of the 2003 IEEE International Conference on Robotics and Automation, Taipei, Taiwan, September 14-19, 2003.

[6] O. Khatib and J. Burdick *"Motion and Force Control of Robot Manipulators"*, IEEE International Conference on Robotics and Automation, 1986.

[7] L. Ljung, *"System Identification Toolbox; User's Guide"*. The MathWorks Inc., Natick, MA, 1991.

[8] K. Nilsson and R. Johansson, *"Integrated architecture for industrial robot programming and control"*. J. Robotics and Autonomous Systems, 29:205-226, 1999.